Capturing multifractality of pressure fluctuations in thermoacoustic systems using fractional-order derivatives

Alan J. Varghese, Aleksei Chechkin, ⓘ Ralf Metzler, and ⓘ R. I. Sujith

View Online   Export Citation   CrossMark

Capturing multifractality of pressure fluctuations in thermoacoustic systems using fractional-order derivatives

Alan J. Varghese,[1] Aleksei Chechkin,[2,a] Ralf Metzler,[2] (ID) and R. I. Sujith[1,b] (ID)

AFFILIATIONS

[1] Department of Aerospace Engineering, IIT Madras, Chennai 600036, India
[2] Institute for Physics and Astronomy, University of Potsdam, 14476 Potsdam-Golm, Germany

[a] **Also at:** Akhiezer Institute for Theoretical Physics, 61108 Kharkov, Ukraine.
[b] **Author to whom correspondence should be addressed:** sujith@iitm.ac.in

ABSTRACT

The stable operation of a turbulent combustor is not completely silent; instead, there is a background of small amplitude aperiodic acoustic fluctuations known as combustion noise. Pressure fluctuations during this state of combustion noise are multifractal due to the presence of multiple temporal scales that contribute to its dynamics. However, existing models are unable to capture the multifractality in the pressure fluctuations. We conjecture an underlying fractional dynamics for the thermoacoustic system and obtain a fractional-order model for pressure fluctuations. The data from this model has remarkable visual similarity to the experimental data and also has a wide multifractal spectrum during the state of combustion noise. Quantitative similarity with the experimental data in terms of the Hurst exponent and the multifractal spectrum is observed during the state of combustion noise. This model is also able to produce pressure fluctuations that are qualitatively similar to the experimental data acquired during intermittency and thermoacoustic instability. Furthermore, we argue that the fractional dynamics vanish as we approach the state of thermoacoustic instability.

Published under license by AIP Publishing. https://doi.org/10.1063/5.0032585

In gas turbine combustors, the coupled interaction between the acoustic field and the heat release rate often leads to a state of large amplitude pressure oscillations, also known as thermoacoustic instability. In turbulent combustors, prior to this state of thermoacoustic instability, there exists a state of intermittency, wherein large amplitude pressure fluctuations occur amidst low amplitude aperiodic pressure fluctuations. Even before this state of intermittency, there is a stable operation regime known as combustion noise, in which the pressure fluctuations are low amplitude and aperiodic. Initially, it was believed that the pressure fluctuations during the state of combustion noise are stochastic in nature. However, it was later shown that the pressure fluctuations during this state are actually deterministic. Further research has shown that multiple scales contribute to the dynamics of the pressure fluctuations during the state of combustion noise. As a result, the multifractal spectrum during combustion noise is wide. Furthermore, the transition from combustion noise to thermoacoustic instability has been interpreted as a loss of multifractality of the pressure fluctuations. However, the existing reduced order models are not able to capture the broad multifractal spectrum seen in experimental data. In this paper, we attempt to construct a model that captures the multifractality of the pressure fluctuations, while faithfully modeling other qualitative and quantitative features.

I. INTRODUCTION

Combustors of gas turbine, ramjet, and rocket engines are prone to a phenomenon known as thermoacoustic instability that arises as a result of the nonlinear coupling between the heat release rate in the combustor and the acoustic field.[1,2] The positive feedback between the flame and the acoustic field can lead to large amplitude pressure oscillations that can cause structural damage to the combustor, overwhelm the thermal protection system, and damage electronic components onboard the payload. Despite decades of active research, an understanding of thermoacoustic instability is far from complete.

As the Reynolds number is increased, the combustor undergoes a transition from a state of combustion noise to thermoacoustic instability.[3] During the state of combustion noise, the pressure fluctuations are low amplitude aperiodic oscillations. This state is also referred to as a state of stable operation. Earlier, it was believed that the state of combustion noise was purely random and hence the origin of the name combustion "noise." Later, Nair et al.[4] and Tony et al.[5] showed that the state of combustion noise is actually deterministic in nature. In contrast, the state of thermoacoustic instability consists of high amplitude oscillations that are periodic in nature. During the occurrence of combustion noise, the low amplitude aperiodic pressure fluctuations display multifractality that indicates that several spatial/temporal scales contribute to its dynamics.[3] However, as the system transitions to the state of thermoacoustic instability, the multifractal manifestations in the temporal features of the system are lost. This loss of multifractality as the system transitions to thermoacoustic instability has also been reported in high fidelity computational fluid dynamics (CFD) simulations.[6] However, reduced order models for pressure fluctuations, which are mainly used in early stages of combustor design, are not able to capture this feature.

A multifractal time series is composed of interwoven fractal subsets with different fractal dimensions.[7] In a multifractal, a number of scaling exponents are required to fully describe the scaling behavior unlike a monofractal whose scaling behavior could be described by the fractal dimension alone. A multifractal spectrum quantifies the multifractality of a time series in terms of the singularity spectrum $f(\alpha)$ and the singularity exponent α. Here, $f(\alpha)$ denotes the dimension of the subset of the series that is characterized by α.[7] The singularity spectrum $f(\alpha)$ is also related to the generalized Hurst exponent H_q via a Legendre transform. The width of the multifractal spectrum gives the range of the scaling exponents present and, therefore, is a measure of the degree of multifractality in the signal.

Of particular interest in this context are two reduced order models: the subcritical Hopf bifurcation model[8] and the kicked oscillator model.[9] In both models, the heat release rate acts as a source term for the acoustic field. In the subcritical Hopf bifurcation model used by Noiray,[8] the heat release rate is modeled as a combination of a third-degree polynomial and an additive white Gaussian noise. In the kicked oscillator model used by Seshadri et al.,[9] the heat release rate is modeled as instantaneous kicks. However, the extent of multifractality seen in these models is very different from that seen in experimental data.

The multifractal spectrum of the pressure fluctuations from these models and that from the experimental data are shown in Fig. 1. Note that the values of the parameters used to generate the data during the occurrence of combustion noise for the Hopf bifurcation model and the kicked oscillator model are the same as that given in Noiray[8] and Seshadri et al.,[9] respectively. The difference in the multifractal spectrum corresponding to the occurrence of combustion noise obtained from the models when compared to that from the experimental data is evident in terms of the asymmetry and the location of the maximum and are tabulated and shown in Table I. We notice that the maxima of the multifractal spectrum during the state of combustion noise in the kicked oscillator model and the Hopf bifurcation model are at a much lower value of α than that for the experimental data. The value α_0 at which the spectrum reaches its maximum is also known as the dominant singularity exponent and a lower value for it indicates that the signal is more periodic. Thus, from Fig. 1, we can deduce that the pressure fluctuations observed in experiments during the state of combustion noise are significantly more aperiodic than those obtained from the models. Another important feature of a multifractal spectrum is its skewness. A right-skewed spectrum indicates more irregularity within the small amplitude temporal structures. In contrast, a left-skewed spectrum indicates higher irregularity within the large amplitude temporal structures. Also, the multifractal spectrum during the state of combustion noise obtained from the models is much more right skewed than that obtained from experimental data (see Table I). Hence, this study aims at developing a reduced order model that captures the multifractal features observed in experiments more faithfully.

As can be seen in the relevant literature, fractal functions are often used to describe complex phenomena characterized by fractal time series.[10] If we try to describe the dynamics of systems with fractal characteristics using conventional integer-order differential
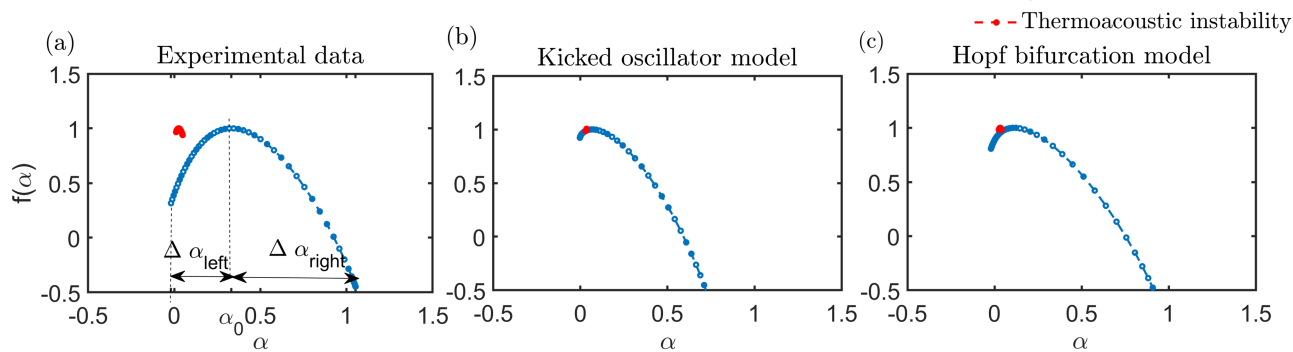

FIG. 1. Multifractal spectra of the pressure fluctuations during combustion noise and thermoacoustic instability from (a) experimental data,[3] (b) the kicked oscillator model,[9] and (c) the Hopf bifurcation model.[8]

TABLE I. Table showing α_0, $\Delta\alpha_{left}$, $\Delta\alpha_{right}$ for the different models discussed. We can observe that the multifractal spectra obtained from the kicked oscillator model and the Hopf bifurcation model are much more right skewed in comparison with the experimental data. Also, the maximum of the $f(\alpha)$ curve during the state of combustion noise occurs at a much higher value of α_0 for the experimental data[3] when compared to the kicked oscillator[9] and Hopf bifurcation models.[8]

Model	α_0	$\Delta\alpha_{left}$	$\Delta\alpha_{right}$
Experimental data[3]	0.332	0.351	0.721
Kicked oscillator model[9]	0.057	0.059	0.653
Hopf bifurcation model[8]	0.113	0.134	0.795

FIG. 2. Schematic of the experimental setup. In order to attain different dynamical states, we vary the Reynolds number as a control parameter.

equations, we see that the integer-order derivatives of the fractal function do not converge. However, a fractional operator of order μ acting on a fractal function of fractal dimension $\mathscr{D}$ yields a new fractal function with fractal dimension $\mathscr{D} + \mu$, where $\mu > 0$ in the case of a derivative and $\mu < 0$ for an integral.[10] In thermoacoustic systems, we observe fractal dynamics, and this motivates us to describe the transition from combustion noise to thermoacoustic instability using fractional-order differential equations.

The work by Richardson[11] also hints at the possibility of fractional-order dynamics in turbulent systems. In this seminal paper, he shows that the mean squared relative displacement between two particles in turbulent flows follows $\langle x^2(t) \rangle = t^3$, in contrast to the t growth for mean square displacement as seen in usual Fickian diffusion. Such deviations from the normal Fickian diffusion are referred to as anomalous diffusion and are, *inter alia*, explained using fractional-order diffusion equations.[12] Moreover, there are numerous articles on the application of fractional calculus to fluid mechanics and turbulence (see, e.g., Refs. 13–16).

In addition to the two main models discussed earlier, there are other interesting variations of these models, with their own peculiar dynamical features, to model thermoacoustic systems. The Hopf bifurcation model[8] considers an additive white Gaussian noise. In reality, there might be temporal correlations present in the forcing term. The paper by Xu *et al.*[17] shows that the Duffing–Van der Pol oscillator forced with colored noise can display stochastic bifurcations. Zhang *et al.*[18] provides a systematic study of the rate-tipping phenomenon in a Duffing–Van der Pol oscillator forced with colored noise. Apart from colored noise, these models could also be forced with fractional Gaussian noise[19] or colored multiplicative noise.[20]

The subcritical Hopf bifurcation model used by Noiray[8] is essentially a classical Van der Pol oscillator, which is forced with additive white noise. In our paper, a fractional-order model for the pressure fluctuations is obtained by fractionalizing the conventionally used forced Van der Pol model. We show that this model captures the presence and the features of multifractality during the state of combustion noise. The outline of the paper is as follows. Section II describes the experimental setup. A brief description of fractional calculus and different definitions of the fractional order derivative are provided in Sec. III. In Sec. IV, we derive the fractional order model for the pressure fluctuations. Section V discusses the numerical simulation scheme used to solve the fractional-order differential equation obtained in Sec. IV. In Sec. VI, we present
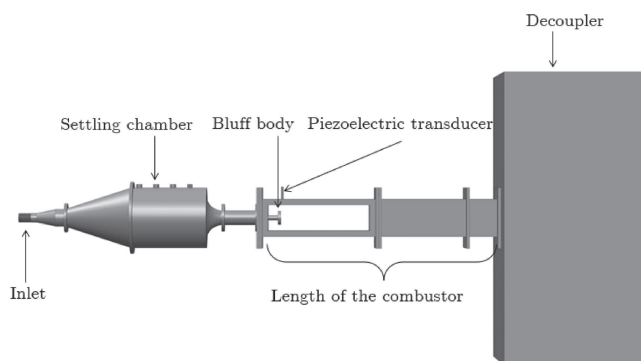
the results and discussion. Finally, concluding remarks are given in Sec. VII.

II. EXPERIMENTAL SETUP

The experiments were performed on a turbulent combustor, the schematic of which is shown in Fig. 2. The experimental setup consists of a settling chamber, a burner, a combustion chamber equipped with a flame holding mechanism, and a decoupler. A circular bluff body with a diameter of 47 mm and a thickness of 10 mm is used as the flame stabilizing mechanism. The bluff body was located 50 mm downstream from the rearward facing step. The length of the combustion chamber was 700 mm. Air partially premixed with fuel [liquified petroleum gas (LPG): butane 60% and propane 40% composition by mass] enters through the inlet, and the reactant mixture gets ignited as it enters the combustion chamber. A more detailed description of the experimental setup can be found in Nair and Sujith,[3] and the data analyzed in this study are the same as that reported in it.

The mass flow rate of fuel and air is controlled using a mass flow controller (Alicat MCR series), which had an uncertainty of $\pm(0.8\%$ of reading $+ 0.2\%$ of full scale reading). Unsteady pressure measurements (p') reported in this study were acquired 90 mm downstream of the rearward facing step using a piezoelectric transducer (sensitivity 72.5 mV kPa^{-1}, 0.48 Pa resolution, and $\pm0.64\%$ uncertainty). The sampling rate of data acquisition is 10 kHz. The data corresponding to combustion noise were acquired at $Re = 1.8 \times 10^4$ and $\phi = 1.1$ and that corresponding to thermoacoustic instability was acquired at $Re = 2.8 \times 10^4$ and $\phi = 0.7$

III. A PRIMER ON FRACTIONAL CALCULUS

Fractional calculus has been widely used in different areas of science. Two of the most important definitions of a fractional derivative are the Riemann–Liouville derivative and the Caputo derivative. The Riemann–Liouville derivative[21–23] of a function $f(t)$ is defined as

follows:

$$
{}^{RL}D_t^\mu f(t) := \begin{cases} \frac{1}{\Gamma(n-\mu)} \frac{d^n}{dt^n}\left[\int_0^t \frac{f(\tau)}{(t-\tau)^{\mu+1-n}} d\tau \right], & n-1 < \mu < n, \\ \frac{d^n}{dt^n} f(t), & \mu = n. \end{cases}
$$

The Caputo fractional derivative[21–23] of a function $f(t)$ is defined as follows:

$$
{}^{C}D_t^\mu f(t) := \begin{cases} \frac{1}{\Gamma(n-\mu)} \int_0^t \frac{1}{(t-\tau)^{\mu+1-n}} \frac{d^n f(\tau)}{d\tau^n} d\tau, & n-1 < \mu < n, \\ \frac{d^n}{dt^n} f(t), & \mu = n. \end{cases}
$$

Here, $\Gamma(.)$ is the gamma function and n is a natural number. The following relation[23] between these two derivatives holds:

$$
{}^{RL}D_t^\mu f(t) = {}^{C}D_t^\mu f(t) + \sum_{k=0}^{n-1} \frac{t^{k-\mu}}{\Gamma(k-\mu+1)} f^{(k)}(0^+),
$$

and therefore, recalling the fractional derivative of the power functions, we have

$$
{}^{RL}D_t^\mu \left(f(t) - \sum_{k=0}^{n-1} \frac{t^{k-\mu}}{\Gamma(k-\mu+1)} f^{(k)}(0^+) \right) = {}^{C}D_t^\mu f(t).
$$

The Caputo definition of the fractional derivative thus incorporates the initial value of the function and of its integer derivatives of lower orders.[23] In applications, the Caputo derivative is preferable for at least two reasons. First, similar to integer derivatives, the fractional Caputo derivative of a constant is still zero, ${}^{C}D_t^\mu (1) \equiv 0$, $\mu > 0$, whereas for the Riemann–Liouville derivative if $\mu \notin \mathbb{N}$ ${}^{RL}D_t^\mu (1) = \frac{t^{-\mu}}{\Gamma(1-\mu)}$, $\mu > 0$. Note that if $\mu \in \mathbb{N}$, the Riemann–Liouville derivative of 1 would be identically 0. Second, the initial conditions for fractional differential equations with Caputo derivatives take on the same form as for integer-order differential equations; i.e., it contain the values of the unknown function and its integer-order derivatives at $t = 0$ contrary to the fractional differential equations with Riemann–Liouville derivatives.[21] In what follows, we use the Caputo fractional derivative. We note that there are various other definitions for a fractional derivative, such as the commonly used Grünwald–Letnikov fractional derivative. The Grünwald–Letnikov fractional derivative of a function $f(t)$ is defined as

$$
{}^{GL}D_t^\mu f(t) = \lim_{h \to 0} \frac{1}{h^\mu} \sum_{k=0}^{\infty} (-1)^k \frac{\Gamma(\mu+1)}{\Gamma(k+1)\Gamma(\mu-k+1)} f(x-kh).
$$

This form is often used in numerical simulations. For sufficiently smooth functions, Grünwald–Letnikov and Riemann–Liouville definitions are equivalent.[21]

The above definitions shows that the fractional-order derivative is a non-local operator; i.e., we need the entire time history from the beginning to evaluate the fractional derivative at a point unlike the integer-order differential operator. Solutions to non-local differential operators would have the influence of memory effects and exhibit so-called aging.[24]

IV. MATHEMATICAL MODELING

Traditionally, the Helmholtz equation is used to model the pressure fluctuations in a combustor of volume V,

$$
\nabla^2 p(x,t) - \frac{1}{c^2} \frac{\partial^2 p(x,t)}{\partial t^2} = -\frac{\gamma-1}{c^2} \frac{\partial Q(x,t)}{\partial t} \quad \text{in the volume } V. \quad (1)
$$

Here, p is the acoustic pressure, c is the speed of sound, and γ is the adiabatic index. The corresponding boundary condition is specified in terms of the acoustic impedance on the surface σ of the combustor, which is defined as follows:

$$
\frac{\tilde{p}(x,s)}{\tilde{u}(x,s) \cdot \hat{n}} = \tilde{Z}(x,s) \quad \text{on the surface } \sigma. \quad (2)
$$

Here, the tilde symbol above a variable denotes the Laplace transform of the corresponding variable, u is the acoustic velocity, and $\hat{n}$ is the unit vector outwardly normal to σ.

In our further analysis, we consider only the dominant eigenmode. We further assume that the acoustic eigenmodes (which are orthogonal) are approximately the same as the thermoacoustic eigenmodes [which are not orthogonal[25] but are the solutions of Eq. (1)] and write the pressure fluctuations and the acoustic velocity in terms of the acoustic eigenmode as follows:

$$
p(x,t) \approx \eta(t)\psi(x), \quad (3a)
$$

$$
u(x,t) \approx -\frac{\nabla\psi(x)}{\rho} \int \eta(t')\, dt'. \quad (3b)
$$

Here, $\psi(x)$ is the dominant acoustic eigenmode and ρ is the density. Since our boundary condition is in the Laplace domain and because it is not easy to analyze the inverse Laplace transform of Eq. (2), we convert Eqs. (1) and (3) into the Laplace domain. Furthermore, we do a spatial averaging to obtain a governing equation for the modal amplitude, which finally yields

$$
\frac{d^2\eta}{dt^2} + \beta \frac{d\eta}{dt} + \omega^2 \eta = \frac{dq}{dt}. \quad (4)
$$

Here,

$$
\beta = \frac{\rho c^2}{V\Lambda} \int_\sigma \frac{\psi(x)^2\, dS}{\tilde{Z}(x,s)}, \quad (5a)
$$

$$
\tilde{q} = \frac{\gamma-1}{c^2} \int_V \tilde{Q}(x,s)\psi(x)\, dV. \quad (5b)
$$

The detailed algebra and the intermediate steps are included in the Appendix. Strictly speaking, β is a function of s, but we assume that it is a constant and hence independent of s. Following Noiray,[8] we decompose the heat release rate fluctuations into a coherent component $\dot{q}_c$ and a non-coherent component $\dot{q}_n$; i.e., $\dot{q} = \dot{q}_c + \dot{q}_n$. Here, q_c is the fluctuation in the heat release due to the feedback of the acoustic field on the flame and is a nonlinear function of η. As a first approximation, the deviation from linearity is assumed to be due to a cubic term, and q_c is modeled as follows:

$$
q_c = \zeta\eta + \frac{\kappa}{3}\eta^3, \quad (6a)
$$

$$
\dot{q}_n = \xi. \quad (6b)
$$

The non-coherent heat release rate fluctuation due to the turbulent nature of the flow field, $\dot{q}_n$, is modeled as a white Gaussian noise ξ of intensity Γ. After substituting Eq. (6) in Eq. (4), we obtain

$$\frac{d^2\eta}{dt^2} + \beta\frac{d\eta}{dt} + \omega^2\eta = (\zeta + \kappa\eta^2)\frac{d\eta}{dt} + \xi. \tag{7}$$

We replace $\beta - \zeta$ with β. Here, β denotes the linear damping present in the system and κ denotes the nonlinear driving present in the system,

$$\frac{d^2\eta}{dt^2} + (\beta - \kappa\eta^2)\frac{d\eta}{dt} + \omega^2\eta = \xi. \tag{8}$$

Equation (8) is similar to a classical Van der Pol oscillator forced with additive white noise. However, the results obtained from this model do not give an adequate description of the experimental results. In order to capture multifractal features of the observed fluctuation phenomena, we propose a minimal fractional generalization of the model. Specifically, we replace the classical van der Pol equation by its fractional counterpart obeying the following integro-differential evolution equation:

$$\frac{d^\mu\eta}{dt^\mu} + (\beta - \kappa\eta^2)\frac{d\eta}{dt} + \omega^\mu\eta = \xi \quad 1 < \mu \le 2. \tag{9}$$

Here, μ is the order of differentiation. Following Duan,[26] we have replaced ω^2 with ω^μ to ensure dimensional consistency and to remove the strong dependency of the fractional order on the dominant frequency of the time series.

A. Intepreting the fractional Van der Pol oscillator model

Here, we provide a physical interpretation for the various parameters that appear in Eq. (9) and how they vary as the system experiences the transition from the state of combustion noise to thermoacoustic instability. The parameters β and κ represent the linear damping and nonlinear driving of the system, respectively. Therefore, these parameters decrease as we approach thermoacoustic instability. The parameters β and κ have certain specific physical units depending on μ. The order of differentiation μ also introduces damping effects in the fractional van der Pol oscillator.[10] The domain $1 < \mu \le 2$ for the fractional order is chosen for reasons of consistency. First, to the best of the authors' knowledge, this is the standard choice of all the papers addressing models of linear and nonlinear fractional oscillators (see, e.g., Refs. 10 and 27–30), and it has a rationale in the subordination concept for developing the fractional Hamiltonian formalism.[10,27] Second, this domain is chosen in the theory of the time-fractional diffusion-wave equation where the time-dependent part (eigendynamics) of the solution obeys the fractional oscillator equation after separation of variables (while for $0 < \mu < 1$, the temporal eigendynamics is strictly decaying).[31–33]

When $\mu = 2$, the model behaves as a classical van der Pol oscillator and no damping effects other than those caused due to the linear and nonlinear damping terms are observed, whereas when μ takes values less than two, we observe damping in the solution. Therefore, as we approach thermoacoustic instability, the value of μ tends to two.

Furthermore, we can rewrite Eq. (9) as a system of equations to obtain

$$\begin{pmatrix} \frac{d\eta}{dt} \\ \frac{d^\mu\eta}{dt^\mu} \end{pmatrix} = \begin{pmatrix} \dot{\eta} \\ \dot{\eta}(\kappa\eta^2 - \beta) - \omega^\mu\eta + \xi \end{pmatrix}. \tag{10}$$

If we were to think of the system of equations in Eq. (10) as governing the motion of an oscillator with η representing its position, we can see that the definition of velocity remains unchanged, whereas it is the equation for acceleration that has the fractional derivative in place of the integer-order derivative, indicating deviation from the Newton's law. A similar type of a fractional van der Pol equation, but without the forcing term, has been used by Periera et al.[29] to model a nonlinear RLC circuit where the capacitance is replaced by a "fractance." Generally, the occurrence of non-localities in time is a standard feature in many complex systems.[12] In our concrete application here, it reflects the contribution of a large range of time scales to the observed dynamics.

V. NUMERICAL SIMULATION SCHEME

We first rewrite Eq. (9) as a multi-order system of equations.[34] We then make use of the Adams–Bashforth–Moulton predictor corrector algorithm[34] to solve this system of equations. We will now summarize this algorithm. Consider the initial value problem,

$$D^\mu y(x) = f(x, y(x)) \quad y^{(k)}(0) = y_0^{(k)}(k = 0, 1, \ldots, \lceil\mu\rceil - 1). \tag{11}$$

Each of the iterates is computed by first performing a prediction step and then performing m-correction steps for this prediction. The algorithm for the predictor step and the corrector step is obtained by replacing the integral operator in the definition of the Caputo fractional derivative with the trapezoidal rule and the rectangular rule, respectively. The algorithm reads as follows:

$$y_{k,0} = \sum_{j=0}^{\lceil\mu\rceil-1} \frac{x_k^j}{j!} y_0^{(j)} + h^\mu \sum_{j=0}^{k-1} b_{jk} f(x_j, y_j), \tag{12}$$

$$y_{k,\nu} = \sum_{j=0}^{\lceil\mu\rceil-1} \frac{x_k^j}{j!} y_0^{(j)} + h^\mu \sum_{j=0}^{k-1} a_{jk} f(x_j, y_j)$$
$$+ h^\mu a_{kk} f(x_k, y_{k,\nu-1}) \quad (\text{where } \nu = 1, 2, \ldots, m). \tag{13}$$

In our simulation, we choose m to be 1. Here,

$$a_{jk} = \frac{1}{\Gamma(2+\mu)} \begin{cases} ((k-1)^{1+\mu} - (k-\mu-1)k^\mu) & \text{if } j = 0, \\ ((k-j+1)^{1+\mu} + (k-j-1)^{1+\mu} - 2(k-j)^{1+\mu}) & \text{if } 1 \le j \le k-1, \\ 1 & \text{if } j = k \end{cases} \tag{14}$$
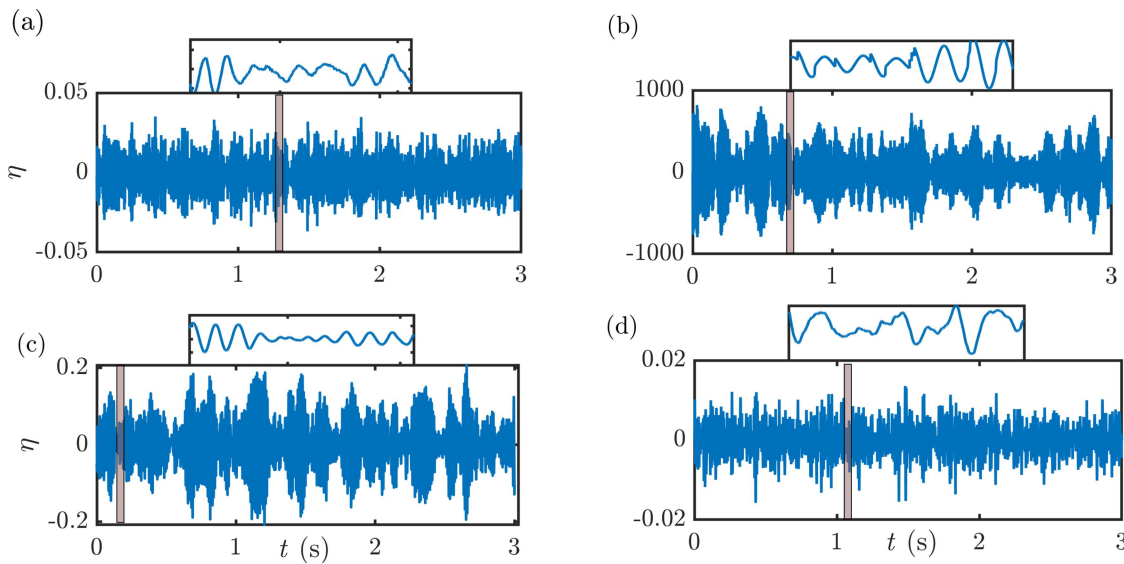
FIG. 3. The pressure fluctuations during the state of combustion noise from (a) experiments, (b) the kicked oscillator model, (c) the Hopf bifurcation (classical Van der Pol forced with white noise) model, and (d) the fractional Van der Pol model. It is evident that qualitative features in the data from the experiment are more closely matched by the data obtained from the fractional Van der Pol model. The experimental data are obtained from the experimental setup detailed in Nair and Sujith[3] with $Re = 1.8 \times 10^4$ and $\phi = 1.1$. The values of the parameters used to generate the data are the same as that given in Noiray[8] and Seshadri et al.[9] The values of various parameters used to generate the data for the fractional Van der Pol model are $\omega = 120$ Hz, $\mu = 1.9$, $\beta = -5$, $\kappa = 25$, and $\Gamma = 10^7$.

and

$$b_{jk} = \frac{1}{\Gamma(1 + \mu)}((k - j)^\mu - (k - 1 - j)^\mu).$$

Equation (9) can be rewritten as a multi-order system of fractional differential equations as follows:

$$D^{1.0}y_1(t) = y_2(t), \quad D^\mu y_2(t) = (\kappa y_1^2 - \beta)y_2 - \omega^\mu y_1 + \xi.$$

The first component y_1 of the solution vector $(y_1, y_2)^T$ of this system, obtained by using the algorithm that we summarized, would be the required solution η of Eq. (9).

VI. RESULTS AND DISCUSSION

In this section, we discuss the results of the numerical simulation corresponding to different dynamical states of the combustor. We also compare the results from the simulation with that from different models and the experimental data corresponding to that state.

The state of combustion noise is characterized by low amplitude aperiodic fluctuations. Figure 3 shows the pressure fluctuations obtained from the experiment[3] and various models.[8,9] We observe that the data from the fractional Van der Pol model closely resemble that from the experiments. The envelope of the pressure fluctuations is very noisy for the experiment, and it is the same for the fractional Van der Pol model. The zoomed-in view of the data from the fractional Van der Pol model has very fine wrinkles similar to those seen in the experimental data. The kicked oscillator model has many sudden non-physical jumps in the pressure fluctuations values, which is

an artifact of modeling the heat release rate as instantaneous kicks. Furthermore, the data from the Hopf bifurcation model (classical Van der Pol forced with white Gaussian noise) tends to be very smooth in the zoomed-in view and lacks the fine wrinkles seen in the experimental data.

Having seen the qualitative similarity between the fractional Van der Pol model and the experimental data, we now proceed to analyze the similarities between the two by making use of various quantitative measures. The Hurst exponent, which is a measure closely related to the fractal dimension of the time series, has been used as a precursor for thermoacoustic instability. The Hurst exponent of the pressure fluctuations in the experimental data during combustion noise is 0.238. The Hurst exponent (H) for the fractional Van der Pol model is 0.254, which is close to that of the experimental data ($H = 0.238$). In contrast, the Hurst exponent of the data from the subcritical Hopf model ($H = 0.077$) and the kicked oscillator model ($H = 0.029$) are very low.

In Fig. 4(a), we show the multifractal spectra of the pressure fluctuations from the fractional Van der Pol model. Here, $\alpha_0 = 0.387$, $\Delta\alpha_{left} = 0.396$, and $\Delta\alpha_{right} = 0.794$. Comparing with Table I, we can observe that the values of these parameters are closer to the experimental data than other models. Most significantly, the value of α_0 corresponding to the peak of the spectrum is larger than that seen in other models and is closer to that seen for the experimental data. As mentioned earlier, a larger value of α_0 indicates that the signal is more aperiodic. Overall, we can observe that the multifractal spectrum from the fractional Van der Pol model looks similar to that of the time series of pressure fluctuations obtained from experiments, which is shown in Fig. 1. The reason for this
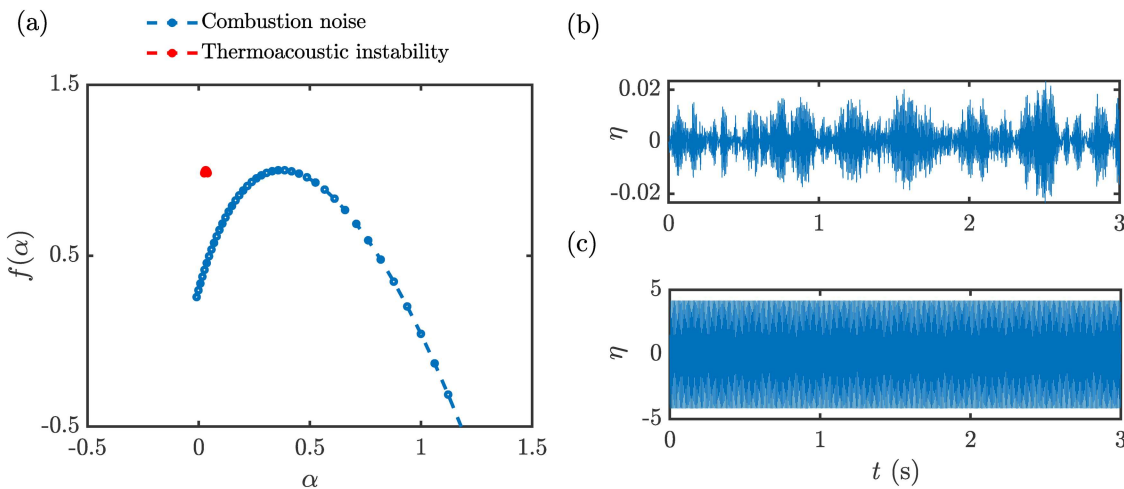
FIG. 4. (a) The multifractal spectra of the pressure fluctuations during the states of combustion noise and thermoacoustic instability from the fractional Van der Pol model. This is the multifractal spectrum obtained for the data generated using the same parameters as mentioned in Fig. 3. Data resembling (b) the state of intermittency generated using the fractional Van der Pol model with parameter values $\omega = 120$ Hz, $\mu = 1.96$, $\beta = -20$, $\kappa = -50$, and $\Gamma = 10^7$ and (c) the state of thermoacoustic instability generated using parameter values $\omega = 120$ Hz, $\mu = 2.0$, $\beta = -10$, $\kappa = -100$, and $\Gamma = 10^7$.

similarity in the multifractal spectrum is the non-local nature of the fractional-order differential operator. In general, multifractality in time series occurs due to two reasons: (i) due to a broad probability density function for the values of the time series and (ii) due to long-range correlations of the small and large fluctuations in time.[7] Nair and Sujith[3] remark that the multifractal nature of the experimental pressure fluctuations is due to the effect of memory rather than the distribution of the data. They verify this claim by showing that randomly shuffling the acquired data results in the loss of multifractality. Our use of fractional operators introduced long-range temporal correlations in the pressure fluctuations and as a result creates multiple temporal scales, which causes a wider multifractal spectrum than that from other models.

In Figs. 4(b) and 4(c), we show the data from the fractional Van der Pol model that resembles the state of intermittency and thermoacoustic instability, respectively. Intermittency is characterized by high amplitude periodic bursts that occur randomly amidst low amplitude aperiodic pressure fluctuations.[35] We are able to obtain the state of intermittency from the model with the order of differentiation, μ less than 2 [$\mu = 1.96$ for the time series shown in Fig. 4(b)]. Usually, the state of intermittency foreshadows thermoacoustic instability.[35] We obtain data similar to thermoacoustic instability with $\mu = 2$ for which the model behaves like a Van der Pol oscillator. Note that we are letting μ tend to 2 as we approach thermoacoustic instability, as discussed earlier. That is, fractional dynamics disappears as we approach thermoacoustic instability, as intuitively expected.

VII. CONCLUDING REMARKS

A fractional-order model for pressure fluctuations is provided in this paper. This model is able to produce data for pressure fluctuations that are strikingly similar to the experimental data during the state of combustion noise. Furthermore, quantitative similarity with the experimental data in terms of the Hurst exponent and the multifractal spectrum is observed. We show that this model captures the multifractality in the pressure fluctuations by making use of fractional-order differential operators that are non-local in time. All of this points to the possibility of having an underlying fractional dynamics. We also obtain data that qualitatively looks similar to the experimental data during the states of intermittency and thermoacoustic instability. In the models, we let μ tend to 2 as we approach thermoacoustic instability; i.e., fractional-order dynamics vanish as we approach instability. The fractional Van der Pol equation could possibly be obtained from considering the fractional form of the Helmholtz equation and will be the topic of future studies. Also, a system identification method that uses the experimental data to estimate the various adjustable parameters used in the fractional-order model needs to be developed.

APPENDIX: SPATIAL AVERAGING

Equations (1) and (3) when represented in the Laplace domain are as follows:

$$\nabla^2 \tilde{p}(x,s) - \frac{s^2}{c^2}\tilde{p}(x,s) = -\frac{(\gamma-1)s}{c^2}\tilde{Q}(x,s) \text{ in the volume } V. \quad \text{(A1)}$$

$$\hat{p}(x,s) \approx \eta(\hat{s})\psi(x), \tag{A2a}$$

$$\hat{u}(x,t) \approx -\frac{\nabla\psi(x)}{s\rho}\tilde{\eta}(t). \tag{A2b}$$

Substituting Eq. (A2a) into Eq. (A1) and then multiplying with the eigenmode $\psi(x)$ and integrating over the volume V, we obtain

$$\tilde{\eta}(s)\left[\int_V \psi(x)\nabla^2\psi(x)\,dV\right] - \frac{s^2}{c^2}\tilde{\eta}(s)\left[\int_V \psi(x)\psi(x)\,dV\right]$$
$$= -s\frac{\gamma-1}{c^2}\int_V \tilde{Q}(x,s)\psi(x)\,dV. \tag{A3}$$

Now, the first term in Eq. (A3) can be simplified as follows:

$$\tilde{\eta}(s)\left[\int_V \psi(x)\nabla^2\psi(x)\,dV\right] = \tilde{\eta}(s)\int_\sigma \psi(x)\nabla\psi(x)\cdot\hat{n}\,dS$$
$$- \tilde{\eta}(s)\int_V \nabla\psi(x)\cdot\nabla\psi(x)\,dV. \tag{A4}$$

From the boundary condition represented in the Laplace domain and Eq. (A2), we obtain

$$\tilde{\eta}(s)\left[\int_V \psi(x)\nabla^2\psi(x)\,dV\right] = -s\tilde{\eta}(s)\rho\int_\sigma \frac{\psi(x)^2\,dS}{\tilde{Z}(x,s)}$$
$$- \tilde{\eta}(s)\int_V \nabla\psi(x)\cdot\nabla\psi(x)\,dV. \tag{A5}$$

Since the acoustic eigenmode is of the form $\psi(x) = e^{-ikx}$, where k is the wave number, it follows that

$$\tilde{\eta}(s)\left[\int_V \psi(x)\nabla^2\psi(x)\,dV\right] = -s\tilde{\eta}(s)\rho\int_\sigma \frac{\psi(x)^2\,dS}{\tilde{Z}(x,s)}$$
$$- k^2\tilde{\eta}(s)\int_V \psi^2(x)\,dV. \tag{A6}$$

Now, substituting Eq. (A6) into Eq. (A3), we finally get

$$-s\tilde{\eta}(s)\rho\int_\sigma \frac{\psi(x)^2\,dS}{\tilde{Z}(x,s)} - k^2\tilde{\eta}(s)\int_V \psi^2(x)\,dV$$
$$-\frac{s^2}{c^2}\tilde{\eta}(s)\left[\int_V \psi(x)\psi(x)\,dV\right] = -\frac{\gamma-1}{c^2}s\int_V \tilde{Q}(x,s)\psi(x)\,dV. \tag{A7}$$

Multiplying Eq. (A7) with c^2 and dividing by $V\Lambda$ (Λ is the mode normalization coefficient), we obtain

$$s^2\tilde{\eta}(s)\underbrace{\frac{1}{V\Lambda}\left[\int_V \psi(x)\psi(x)\,dV\right]}_{1} + s\tilde{\eta}(s)\underbrace{\frac{\rho c^2}{V\Lambda}\int_\sigma \frac{\psi(x)^2\,dS}{\tilde{Z}(x,s)}}_{\beta}$$
$$+ \omega^2\tilde{\eta}(s)\underbrace{\frac{1}{V\Lambda}\left[\int_V \psi(x)\psi(x)\,dV\right]}_{1}$$
$$= s\frac{\gamma-1}{c^2}\underbrace{\int_V \tilde{Q}(x,s)\psi(x)\,dV}_{\tilde{q}}. \tag{A8}$$

Now, representing the above equation in the time domain, we get

$$\frac{d^2\eta}{dt^2} + \beta\frac{d\eta}{dt} + \omega^2\eta = \frac{dq}{dt}. \tag{A9}$$

DATA AVAILABILITY

The data that support the findings of this study are available from the corresponding author upon reasonable request.

REFERENCES

[1] T. Lieuwen, *Unsteady Combustor Physics* (Cambridge University Press, 2012).

[2] R. I. Sujith and V. R. Unni, "Complex system approach to investigate and mitigate thermoacoustic instability in turbulent combustors," Phys. Fluids **32**, 061401 (2020).

[3] V. Nair and R. I. Sujith, "Multifractality in combustion noise: Predicting an impending combustion instability," J. Fluid Mech. **747**, 635–655 (2014).

[4] V. Nair, G. Thampi, S. Karuppusamy, S. Gopalan, and R. Sujith, "Loss of chaos in combustion noise as a precursor of impending combustion instability," Int. J. Spray Combust. Dyn. **5**, 273–290 (2013).

[5] J. Tony, E. Gopalakrishnan, E. Sreelekha, and R. I. Sujith, "Detecting deterministic nature of pressure measurements from a turbulent combustor," Phys. Rev. E **92**, 062902 (2015).

[6] M. Kamin, J. Mathew, and R. I. Sujith, "A numerical study of an acoustic–hydrodynamic system exhibiting an intermittent prelude to instability," Int. J. Aeroacoust. **18**, 536–553 (2019).

[7] J. W. Kantelhardt, S. A. Zschiegner, E. Koscielny-Bunde, S. Havlin, A. Bunde, and H. Stanley, "Multifractal detrended fluctuation analysis of nonstationary time series," Physica A **316**, 87–114 (2002).

[8] N. Noiray, "Linear growth rate estimation from dynamics and statistics of acoustic signal envelope in turbulent combustors," J. Eng. Gas Turbine. Power **139**, 041503 (2017).

[9] A. Seshadri, V. Nair, and R. I. Sujith, "A reduced-order deterministic model describing an intermittency route to combustion instability," Combust. Theory Modell. **20**, 441–456 (2016).

[10] B. J. West, "Fractal physiology and the fractional calculus: A perspective," Front. Physiol. **1**, 12 (2010).

[11] L. F. Richardson, "Atmospheric diffusion shown on a distance-neighbour graph," Proc. R. Soc. Lond. Ser. A **110**, 709–737 (1926).

[12] R. Metzler, J.-H. Jeon, A. Cherstvy, and E. Barkai, "Anomalous diffusion models and their properties: Non-stationarity, non-ergodicity, and ageing at the centenary of single particle tracking," Phys. Chem. Chem. Phys. **16**, 24128–24164 (2014).

[13] V. V. Kulish and J. L. Lage, "Application of fractional calculus to fluid mechanics," J. Fluids Eng. **124**, 803–806 (2002).

[14] D. del Castillo-Negrete, B. Carreras, and V. Lynch, "Fractional diffusion in plasma turbulence," Phys. Plasmas **11**, 3854–3864 (2004).

[15] Y. Zhou and L. Peng, "On the time-fractional Navier–Stokes equations," Comput. Math. Appl. **73**, 874–891 (2017).

[16] G. Boffetta and I. Sokolov, "Relative dispersion in fully developed turbulence: The Richardson's law and intermittency corrections," Phys. Rev. Lett. **88**, 094501 (2002).

[17] Y. Xu, R. Gu, H. Zhang, W. Xu, and J. Duan, "Stochastic bifurcations in a bistable Duffing-van der Pol oscillator with colored noise," Phys. Rev. E **83**, 056215 (2011).

[18] X. Zhang, Y. Xu, Q. Liu, and J. Kurths, "Rate-dependent tipping-delay phenomenon in a thermoacoustic system with colored noise," Sci. China Technol. Sci. **63**, 2315–2327 (2020).

[19] R. Mei, Y. Xu, and J. Kurths, "Transport and escape in a deformable channel driven by fractional Gaussian noise," Phys. Rev. E **100**, 022114 (2019).

[20] Y. Xu, X. Liu, Y. Li, and R. Metzler, "Heterogeneous diffusion processes and nonergodicity with Gaussian colored noise in layered diffusivity landscapes," Phys. Rev. E **102**, 062106 (2020).

[21] I. Podlubny, *Fractional Differential Equations: An Introduction to Fractional Derivatives, Fractional Differential Equations, to Methods of Their Solution and Some of Their Applications* (Elsevier, 1998).

[22] K. Oldham and J. Spanier, *The Fractional Calculus Theory and Applications of Differentiation and Integration to Arbitrary Order* (Elsevier, 1974).

[23] R. Gorenflo and F. Mainardi, "Fractional calculus: Integral and differential equations of fractional order," in *Fractals and Fractional Calculus in Continuum Mechanics* (Springer-Verlag, Wien, 1997), pp. 223–276.

[24] J. H. Schulz, E. Barkai, and R. Metzler, "Aging renewal theory and application to random walks," Phys. Rev. X **4**, 011028 (2014).

[25] K. Balasubramanian and R. I. Sujith, "Thermoacoustic instability in a Rijke tube: Non-normality and nonlinearity," Phys. Fluids **20**, 044103 (2008).

[26] J.-S. Duan, "The periodic solution of fractional oscillation equation with periodic input," Adv. Math. Phys. **2013**, 869484.

[27] A. Stanislavsky, "Fractional oscillator," Phys. Rev. E **70**, 051103 (2004).

[28] R. S. Barbosa, J. T. Machado, B. M. Vinagre, and A. J. Calderon, "Analysis of the van der Pol oscillator containing derivatives of fractional order," J. Vib. Control **13**, 1291–1301 (2007).

[29] E. Periera, C. A. Monje, B. M. Vinagre, and F. Gordillho, "Matlab toolbox for the analysis of fractional order systems with hard nonlinearities," in Proceedings of First IFAC Workshop on Fractional Differentiation and Its Application (FDA'04), Bordeaux, France (2004).

[30] A. Al-rabtah, V. S. Ertürk, and S. Momani, "Solutions of a fractional oscillator by using differential transform method," Comput. Math. Appl. **59**, 1356–1362 (2010).

[31] F. Mainardi, "The time fractional diffusion-wave equation," Radiophys. Quantum Electron. **38**, 13–24 (1995).

[32] Y. Luchko, "Fractional wave equation and damped waves," J. Math. Phys. **54**, 031505 (2013).

[33] W. R. Schneider and W. Wyss, "Fractional diffusion and wave equations," J. Math. Phys. **30**, 134–144 (1989).

[34] K. Diethelm, D. Baleanu, and E. Scalas, *Fractional Calculus: Models and Numerical Methods* (World Scientific, 2012).

[35] V. Nair, G. Thampi, and R. I. Sujith, "Intermittency route to thermoacoustic instability in turbulent combustors," J. Fluid Mech. **756**, 470–487 (2014).